Journal of the Iranian Chemical Society (2018) 15:2401–2410
https://doi.org/10.1007/s13738-018-1429-5

ORIGINAL PAPER

Chrysin/β-cyclodextrin supramolecular system: a quantum mechanical investigation

Mina Ghiasi[1] · Narjes Gerayeli[2] · Mohsen Tafazzoli[2]

Received: 20 February 2017 / Accepted: 2 June 2018 / Published online: 24 July 2018

Abstract
Chrysin is a bioflavonoid which possesses a wide range of important biological activities. In present study, we used a quantum mechanical approach to shed light on the antioxidant ability and antioxidant mechanism of chrysin to scavenge hydroxyl radical (˙OH) in solution phase. The analysis of the theoretical bond dissociation enthalpy (BDE) values and spin density of the radicals to determine the delocalization possibilities at B3LYP/6-311++G** level clearly shows the importance of the A-ring and the 7-OH group in antioxidant reactivity. In the next step, the inclusion of chrysin with β-CD has been investigated extensively using theoretical methods. Density functional theory (M05-2X) employing the 6–31+G* basis set has been used to research the lowest energy geometry for all studied complexes in gas and water mediums. The results of calculations show that the A ring of chrysin with large cavity side of β-CD significantly formed the favorable β-CD/chrysin complex in both phases. Our observations also inferred that hydrogen bonds were the key interactions which stabilized the chrysin/β-CD complex. We used Bader's atoms in molecules (AIM) theory to perform a topological study on chrysin/β-CD complex to emphasize the hydrogen bonds. According to our findings, the process of inclusion increased not only the solubility of chrysin but also its antioxidant potential.

Keywords Cyclodextrin · Chrysin · Binding energy · Inclusion complex · QM calculation

Introduction

Cyclodextrins (CDs) are cyclic oligosaccharides built up from α-D-glucopyranose units connected with a α-1, 4 glycosidic linkage. CD with lipophilic inner cavities and hydrophilic outer surface could interact with a large variety of guest compounds to form inclusion complex [1–3], Fig. 1. Cyclodextrins have been used as pharmaceutical carrier to increase the solubility, stability, and bioavailability of poor water-soluble drugs by the formation of an inclusion complex between the host cyclodextrin molecule and the guest drug molecule [4–10]. During the complex formation with drug molecules, no covalent bonds exist between the CD and its guest, thus complexation can be considered as a dynamic process [11]. Between different forms of CDs, α-CD, β-CD and γ-CD, β-CD has been widely used in the pharmaceutical applications because of its availability and cavity size which is suitable for the wide range of drugs [12].

Bioflavonoids are benzo-gamma-pyrone derivatives of plant origin with wide range of physiological activities such as antimicrobial, anti-inflammatory, and antiallergenic compounds which can prevent biological and chemical substances from oxidative damage by reactive oxygen species (ROS) such as hydroxyl radical (˙OH), superoxide radical ($O2^{-\bullet}$), singlet oxygen, and lipid proxy-radicals [13, 14]. Chrysin (5, 7-dihydroxyflavone), Fig. 2, is a non-toxic bioflavonoid that possess many biological activities and pharmacological effects [15, 16]. Chrysin has commonly been used in human medicine for the treatment of human prostate cancer [17] therefore, it has less toxicity for human body and has the potential to be novel.

Therefore, the objectives of this study were to investigate the antioxidant mechanism of chrysin, including hydroxyl radical scavenging activity. Since the solubility of chrysin in aqueous solution is low, therefore, the inclusion complex of chrysin with beta-CD was studied to improve the solubility and the stability of chrysin in

✉ Mina Ghiasi
ghiasi@alzahra.ac.ir

[1] Department of Chemistry, Faculty of Physics and Chemistry, Alzahra University, Vanak, Tehran, PO Box 19835-389, Iran

[2] Department of Chemistry, Sharif University of Technology, Tehran, PO Box 11365-9516, Iran

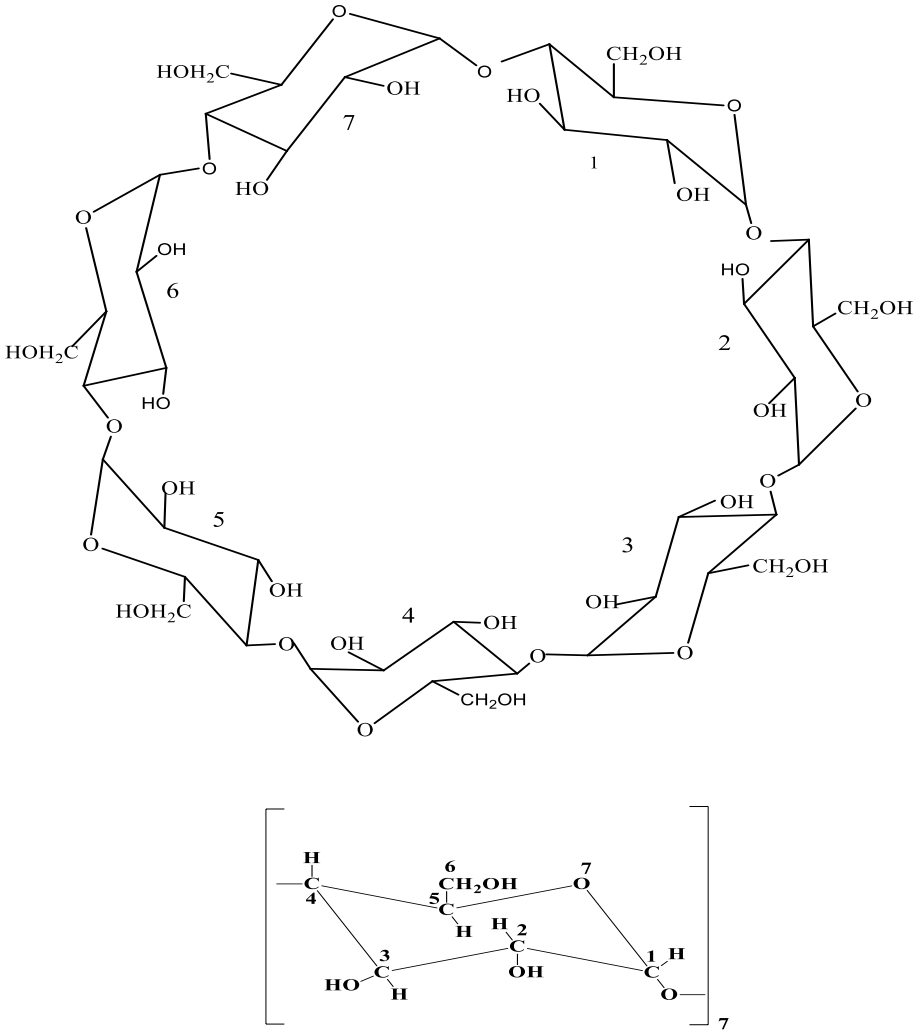

Fig. 1 Chemical structure of β-CD with numbering for key atoms

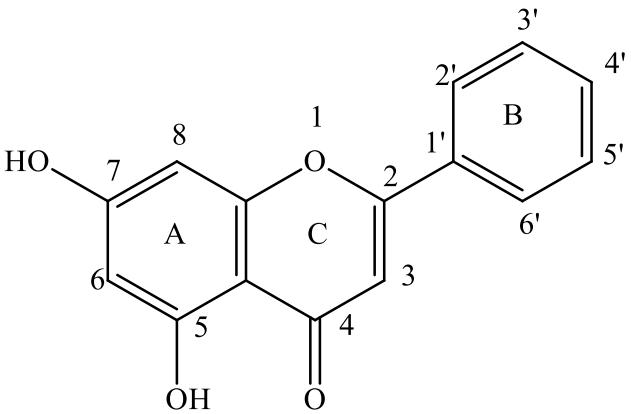

Fig. 2 Chemical structure of chrysin with numbering for some key atoms

aqueous solution [17]. Chakraborty, Zhu and their colleagues have studied that the solubility of chrysin could be improved by encapsulating within β-CD [19, 20]. The process of inclusion increased not only the solubility of chrysin but also its antioxidant potential activity [19]. With this goal toward increasing our knowledge about supramolecular interaction, we focus on the O–H…O interactions between host and guest molecules and the conformational changes of the guest molecule. In addition, the effects of the inclusion on the antioxidant ability and on its chemical and stability have been determined.

There are many uses for applying computational chemistry to the study of CD, especially in the structural characterization of host–guest complexes by ab initio [21] molecular mechanics (MM) [22] molecular dynamics (MD) [23] Semiempirical methods (PM3, MNDO AM1, etc.) [24] and ONIOM methods [25] To our knowledge, due to the size of these systems quantum mechanical calculations consisted of DFT method employing high-level basis set on CDs have not been reported. Thus, the main aim of the present work is characterization of the structural details of β-CD, chrysin and chrysin/β-CD complex using high-level DFT calculations.

Computational details

All calculations were carried out with the Gaussian 09 [26] as basic program, HYPER CHEM version 7.0 [27] and Gaussian Viewer [28] as graphical medium. The optimization of the geometries for chrysin and its radicals were performed by employing a hybrid Hartree–Fock-density functional scheme, the adiabatic connection method—Becke three-parameter with Lee–Yang–Parr (B3LYP) functional of density functional theory (DFT) [29] employing the standard basis set 6-311++G**. Full optimizations were performed without any symmetry constrains. We computed the harmonic vibrational frequencies to confirm that an optimized geometry correctly corresponds to a local minimum which has only real frequencies. QST3 method was used to search for transition state. Transition state geometry was rechecked using IRC and FREQ calculations. In continuation, to optimize the chrysin/β-CD complex, M05-2X [30, 31] method employing 6–31+G* basis set has been used. According to Zhao et al. this method is suitable for structures with weak bonds such as hydrogen bonds. The AIM analysis has been performed with the AIM2000 code [32] with all default options to clarify the hydrogen bond interactions. The solvent effects were investigated using polarized continuum (overlapping spheres) model (PCM) of Tomasi and coworkers [33, 34] at the M05-2X/6–31+G* level for water solvent. Also, all energies have been corrected for the basis set superposition error (BSSE) using the Boys and Bernardi method [35].

The coordinate system has been used to define the complexation process presented in Fig. 3. The β-CD ring were constructed with seven glucose units positioned symmetrically around the *X*-axis so all the glycosidic oxygen atoms of β-CD were placed on to the ZY plane and their mass center were defined as the center of the coordination system. The C1′–C2 inter cyclic bond of chrysin is along X-axis and the guest position is determined by X coordinate of the C1 carbon atom considered as reference atom. The inclusion complexation was emulated by moving the guest molecule (chrysin) from −7 to +7 Å along the *X*-axis at fixed increment of 0.5 Å in the two defined orientations, Fig. 3. Four starting positions were generated by movement of the C1′–C2 bond along the *X*-axis from the large side and small side of β-CD at a distance of 7 Å (+X,) and −7 Å (−X,) from two positions, B ring and A–C ring, Fig. 3. The geometry generated at each step is then optimized allowing changes from the initial conformations but keeping the movement of the reference atom and β-CD totally restricted. To find more stable structure of the complex, chrysin was rotated in the cavity around the *x*-axis at 20 intervals from 0 to 360 and each complex was re-optimized without imposing any restrictions.

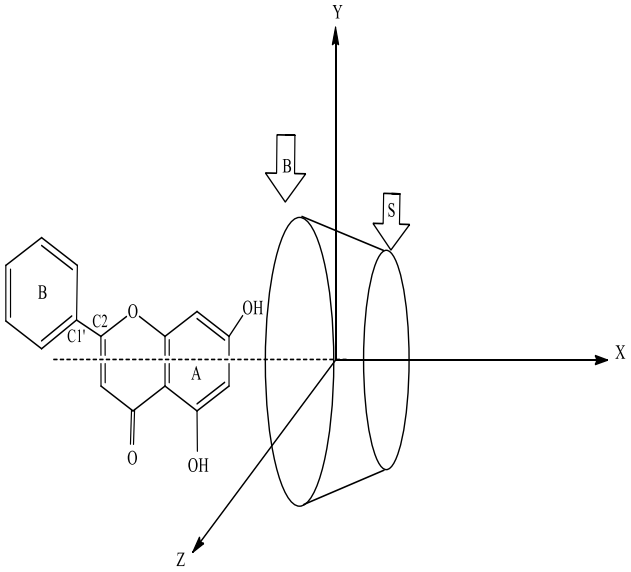

Fig. 3 Coordinate systems used to define the process of complexion from different positions

Theoretical parameters

Calculation of bond dissociation enthalpy and spin distribution

A theoretical, quantum chemically determined, suitable parameter for describing the abstraction of a hydrogen radical from O–H bond is the difference in enthalpy of the flavonoid (FLOH) and its corresponding radical (FLO$^{\cdot}$), bond dissociation enthalpy (BDE). The BDE is equal to $H_r + H_h - H_p$ where H_r is the enthalpy of the radical generated by H-abstraction, H_h is the enthalpy of the H atom and H_p is the enthalpy of the parent molecule, reaction 1.

$$\mathrm{FLOH} + {}^{\cdot}\mathrm{OH} \rightarrow \mathrm{FLO}^{\cdot} + \mathrm{H_2O} \quad (1)$$

The FLO$^{\cdot}$ formed radical must be relatively stable so this reaction is thermodynamically favorable. BDE values were corrected to take in to account the zero point energy and the contributions from translational, rotational, and vibrational degrees of freedom in the heat of reaction at 298 K.

To gain insight to the delocalization possibilities of chrysin, which are the reason for its antioxidant activity, spin distributions were calculated for the different radicals of chrysin after BDE calculation for chrysin. Afterwards, hydroxyl radical scavenging mechanism by chrysin was discussed.

The results of previous studies to obtain an accurate description of the BDE in phenolic compounds show that the DFT method with 6-311++G** basis set is sufficient to give an accurate description of the BDE [36–40]. Hence, we used this method for continuation of our study.

Calculation of ionization potential

Ionization potential is the second suitable parameter to describe the antioxidant activity of flavonoids, Eq. 2.

$$FLOH + {}^{\cdot}OH \rightarrow FLOH^{\cdot+} + OH^{-} \rightarrow FLO^{\cdot} + H_2O \quad (2)$$

According to reaction (2), electron transfers from the molecule to the radical, lead to indirect hydrogen abstraction. The electron-giving ability of the antioxidant compounds is very well correlated to the highest occupied molecular orbital energy (E_{HOMO}) according to Koopman's theorem [40, 41].

$$IP\ (Ionization\ potential) = -HOMO\ energy \quad (3)$$

Results and discussion

Geometry optimization of chrysin and calculation of E_{HOMO}

Chrysin structure was fully optimized at B3LYP method using 6-311++G** basis set with no initial symmetry restrictions and assuming C_1 point group. Figure S1 shows the optimized structure of chrysin as well as its HOMO orbital. As Fig. S1 demonstrates, the HOMO is localized on the A–C ring of chrysin molecule and calculated E_{HOMO} is equal to − 7.83 ev. Also some structural details of chrysin molecule are depicted in Table 1.

BDE values of optimized chrysin

Geometrical optimizations on the radicals were performed in the solution, starting from the optimized structure of the parent molecule, after the H-atom was removed from the 5 and 7 positions with UB_3LYP/6-311++G** method. Some structural details of both radicals are presented in Table 1. Also, calculated BDE values for two radicals formed by H-abstraction on chrysin using UB_3LYP/6-311++G**method show the following BDE sequence for the OH groups: 7-OH (76.88 kcal/mol) < 5-OH (87.91 kcal/mol). As expected, the BDE value for 5-OH group because of internal hydrogen bonding is highly thermodynamically unfavorable, so it has the highest value, 87.91 Kcal/mol. These results clearly confirm that H transfer is energetically favorable from the A-ring, especially from 7 positions. Therefore, the A-ring is the most important site for H-transfer and consequently for the antioxidant capacity.

Table 1 Some structural details of optimized chrysin and related radicals geometry at B3LYP/6-311++G** level in gas phase

Connected atoms	Chrysin	Radical of 5 position OH	Radical of 7 position OH
B3LYP/6-311++G**			
Bond distance (Å)			
C2–C1′	1.47	1.47	1.47
C4–C3	1.44	1.46	1.44
O1–C2	1.36	1.37	1.35
C5–C6	1.39	1.46	1.38
C1′–C2′	1.40	1.40	1.40
Bond angel (°)			
O1–C2–C1′	112.30	112.38	112.53
C3–C2–C1′	125.92	126.78	125.85
C6′–C1′–C2′	118.87	118.85	118.95
C2–C3–C4	121.55	123.37	121.92
Dihedral angel (°)			
O1–C2–C3–C4	− 179.97	− 1.41	− 0.99
O1–C2–C1′–C2′	− 20.78	− 20.85	160.97
C3–C2–C1′–C6′	− 21.46	158.23	159.88

Comparison between the spin densities of the radicals formed from the A-ring

Within an unrestricted scheme, the spin density is often considered to be a more realistic parameter and provides a better representation of the reactivity [42]. The importance of the spin density for the description of flavonoids has been pointed out by the recent paper of Leopoldini et al. [43]. Π-electron delocalization leads to the stabilization of the radicals obtained after H-abstraction. To understand the relationship between the electron delocalization and the reactivity of the radicals, one can examine the electron distribution in the highest occupied molecular orbital (HOMO). Armed with these back grounds, we decided to analyze the spin density on the different form of chrysin radicals. The HOMO shapes of two radicals is presented in Fig. 4. As depicted in Fig. 4, the HOMO shape for the two radicals (corresponding to H-removal from one of the two OH groups) exhibits sufficient variations for explaining the differences in activity between those OH groups.

Calculated net charges and spin distribution of different radicals after H abstracting from chrysin are presented in Table 2. These partial charges and spin densities were derived from NBO (natural bond orbital) calculation.

Table 2 indicates that the spin population on the remaining O-atom after H-removal and on the neighboring C-atoms appears to be slightly more delocalized for radicals issued from the A-ring (7-OH position). For example, the spin density on the O (C7) for radical of 7-OH position and radical of 5-OH position is 0.42 and − 0.01, respectively.

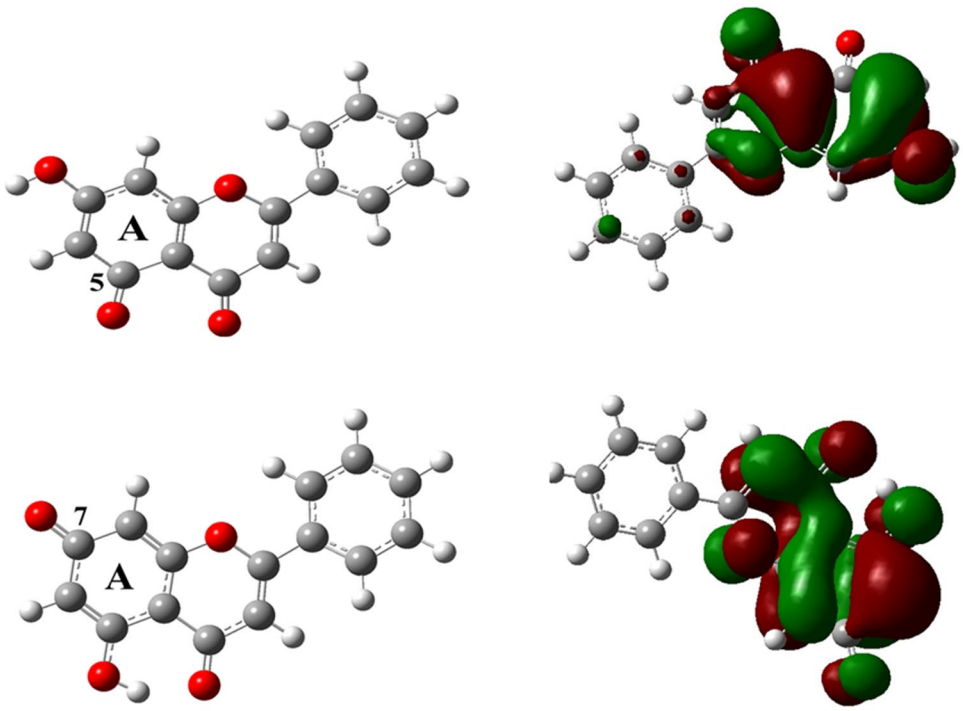

Fig. 4 Optimized structure of chrysin radicals and their HOMO orbital at B3LYP/6-311++G** level in gas phase

Table 2 Comparison between derived net atomic charges and unpaired spin distributions for different radicals of chrysin by B_3LYP/6-311++G** method

Atomic number	Net charge		Spin density	
	Radical of 5 position OH	Radical of 7 position OH	Radical of 5 position OH	Radical of 7 position OH
C5	−0.60	−0.30	−0.12	−O.13
O (C5)	−0.19	−0.27	0.37	−0.02
C6	0.83	0.69	0.37	0.26
C7	−0.83	−0.70	−0.16	−0.09
O (C7)	−0.21	−0.22	−0.01	0.42
C8	−0.44	−0.66	0.46	0.34
O1	0.04	0.04	0.01	0.00
O (C4)	−0.26	−0.32	0.01	0.06

It must be stressed that the more delocalized spin density in the radical, the easier the formation of radical lead to and the lower BDE make [44]. As a consequence, the BDE is lower for 7-OH than 5-OH.

Mechanism of chrysin antioxidant activity

According to recent experimental studies, the antimutagenic activity of phenolic compounds, particularly flavonoids such as chrysin, is based on their scavenging capacity of hydroxyl radical (˙OH) [45]. Since the mechanisms and the sequence of events by which free radicals are not fully understood, we focused on the reaction path when the hydroxyl radical attacks to the chrysin molecule.

Hydroxyl radical scavenging mechanism

The hydroxyl radical (˙OH) in the cells can easily cross cell membranes at specific sites, react with most biomolecules and furthermore cause tissue damage and cell death. Thus, removing ˙OH is very important for the protection of living systems.

From proceeding discussion regarding BDE and charge density distribution, we have considered that the 7-OH is the most suitable site for ˙OH attack. Compound that might arise from addition of ˙OH to the chrysin is called intermediate. Product of this reaction results from the 7-OH bond cleavage in intermediate. Geometry of product and intermediate was optimized at the UB_3LYP/6-311++G** level and presented in Fig. 5.

Efforts to find a transition state geometry between intermediate and reactants or products was fruitless. Therefore, it is expected that the attack of hydroxyl radical is carried directly on hydrogen atom adjacent to oxygen atom connected to C7. An energy diagram has been drawn for this reaction schematically in Fig. 5. As Fig. 5 reveals, relative energy values suggest that this reaction is exothermic by about − 26.66 kcal/mol.

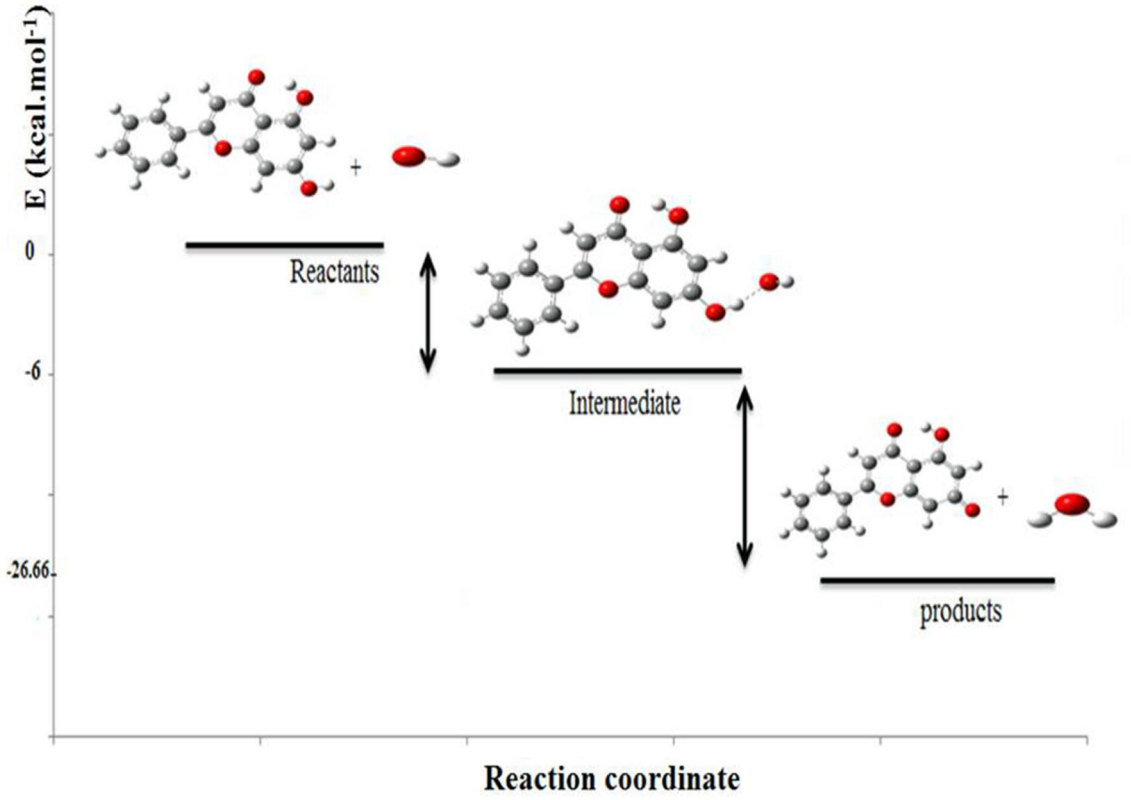

Fig. 5 Energy diagram for the reaction of hydroxyl radical attack to the chrysin molecule at B3LYP/6-311++G** level in gas phase

Geometry optimization of β- cyclodextrin

Molecular structure of β-CD was built from their corresponding X-ray coordinates [46]. Gaussian viewer were used to convert CSD coordinate files into PDB files and add hydrogen in idealized positions in structures. Figure S2 shows the optimized structure of β-CD from different

Table 3 Some structural details of optimized β-CD in water solvent at M05-2x/6–31+G* level

M05-2x/6–31+G*	
Connected atoms	Bond distance (Å)
C1–C2	1.52–1.53
C5–O	1.46–1.48
C4–C5	1.52–1.53
C4–C3	1.51–1.52
C3-O(C3)	1.43–1.44
C2–O(C2)	1.42–1.45
Connected atoms	Bond angel (°)
C1–O–C4	118.35–119.49
C1–C2–C3	109.04–110.75
C4–C5–O	103.72–107.57
Connected atoms	Dihedral angel(°)
C5–O–C1–O	58.31–61.58
O(C2)–C2–C3–O(C3)	62.06–69.00

views. Some structural details of β-CD are presented in Table 3 in water solvent at M05-2x /6–31+G* level.

Calculation of binding energy

To qualify the interaction between host and guest in the optimized geometries, the binding energy (BE) is evaluated using Eq. 4 [20, 47].

$$\mathrm{BE} = E_{\mathrm{Chrysin}/\beta-\mathrm{CD}} - \left(E_{\mathrm{isolated\ Chrysin}} + E_{\mathrm{isolated}\beta-\mathrm{CD}}\right) \quad (4)$$

According to Eq. (4), BE is the binding energy, $E_{\mathrm{Chrysin/\beta\text{-}CD}}$ is the energy of complex, and $(E_{\mathrm{isolated\ Chrysin}} + E_{\mathrm{isolated\ \beta\text{-}CD}})$ is the sum of energies of free β-CD and chrysin molecules. The structure with the lowest binding energy was considered as the best one.

The binding energy was calculated at the same level with correction for the basis set superposition error (BSSE) using the Boys–Bernardi counterpoise (CP) technique.

Binding energy of the chrysin/β-CD complex

The optimized chrysin molecule was docked into optimized β-CD model. Four possible orientations were considered in Fig. 3: (1) the A ring of chrysin molecule orientated to the center of mass of β-CD from the big size cavity, namely AB, (2) the B-ring orientated to the center of mass of β-CD from the big size cavity, namely BB, (3) the A ring of chrysin molecule orientated to the center of mass of β-CD from the small size cavity, namely AS, (4) the B-ring orientated to the center of mass of β-CD from the small size cavity, namely BS. Multiple starting positions were generated by movement of the bound along the *X*-axis, and complexes with the B and A ring in to X space were build. The relative position between the host (β-CD) and the guest (chrysin) was measured by the X-coordinate of the labeled carbon atoms of the guest, Fig. 3. To find more stable geometry of these complexes, the distance between label atoms, was scanning trough the X-direction to 7 Å with a step of 0.5 Å. The structure generated at each step is optimized. Figure 6 depicted the various possible structures of β-CD/chrysin inclusion complexes. Table 4 shows the calculated binding energy (BE) of complexed chrysin with β-CD in gas phase included the BSSE-CP correction and in water phase at

Table 4 Calculated binding energy (BE) of chrysin complexed with β-CD in gas and water solvent at M05-2x/6–31+G* level with the BSSE-CP correction

Inclusion complex	BE (kcal/mol)	
	Gas phase	Water phase
AB	−23.79	−33.27
BB	−20.62	−25.45
AS	−11.16	−24.31
BS	−10.22	−17.22

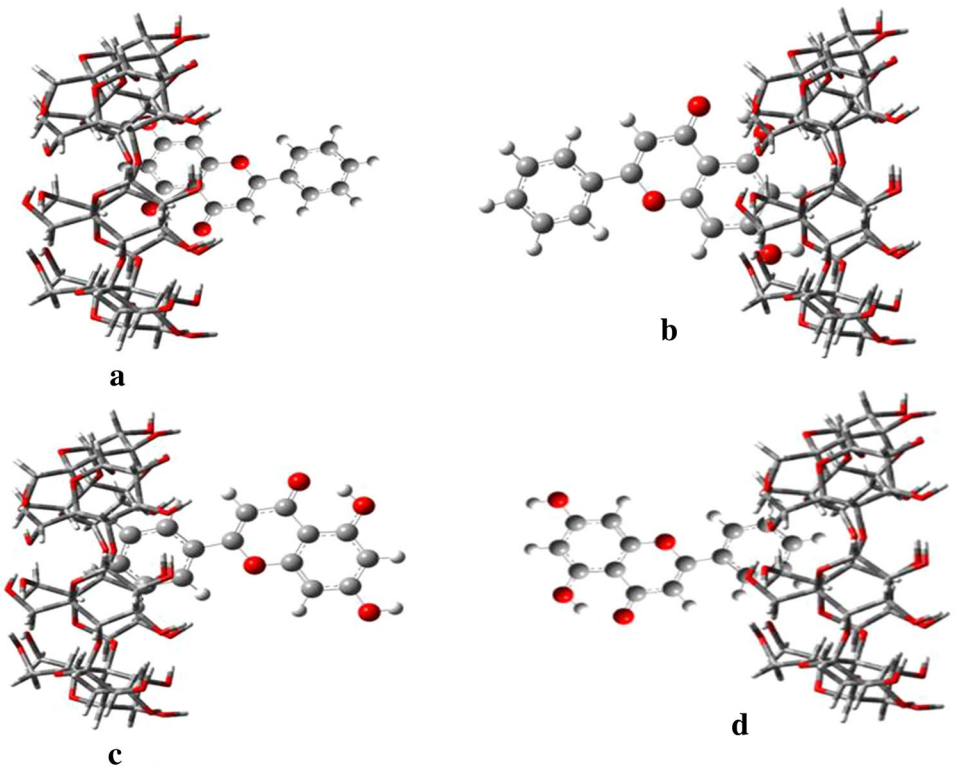

Fig. 6 Various possible structures of β-CD/chrysin inclusion complexes: **a** A ring/big size cavity of β-CD(AB), **b** A ring/small size cavity of β-CD(AS), **c** B ring/big size cavity of β-CD(BB), **d** B ring/small size cavity of β-CD(BS)

Table 5 Position, length and bond angles of hydrogen bonds in AB complex in water solvent at M05-2X/6–31+G*

The number of α-D-glucopyranoside	Atom of chrysin	Atom of βCD	Length of hydrogen bond (A)	Atoms of hydrogen bonding angel	Bonding angel involving hydrogen bonds (°)
1	H(C6)	O(C6)	2.65	C6–H(C6)–O(C6)	170.00
2	H(O–C7)	O(C6)	1.72	C7–H(O–C7)–O(C6)	162.46
3	O(C7)	H(C5)	2.38	O(C7)–H(C5)–C5	145.60
5	O1	H(C3)	2.70	O1–H(C3)–C3	84.13
6	O(C4)	H(O–C3)	1.91	O(C4)–H(O–C3)–O(C3)	158.34
6	O(C4)	H(C3)	2.68	O(C4)–H(C3)–C3	112.51
6	O(C5)	H(C3)	2.77	O(C5)–H(C3)–C3	134.30
6	O(C5)	H(C5)	2.43	O(C5)–H(C5)–C5	143.72
7	O(C5)	H(C3)	2.67	O(C5)–H(C3)–C3	147.88
7	O(C5)	H(C5)	2.59	O(C5)–H(C5)–C5	153.23

Table 6 Comparison of some structural details between single molecule of chrysin and chrysin/ β-CD complex (AB) in water solvent at M05 2X/6–31+G* level

Connected atom	Bond distance (Å) In chrysin/β-CD	Bond distance (Å) in chrysin
O4–H(O–C5)	1.74	1.71
H–O(C5)	0.99	0.99
C7–OH	1.34	1.35
H–O(C7)	0.99	0.97

M05-2x/6–31+G* level of calculation. The negative binding energy (BE) changes upon complexation clearly demonstrate that β-CD can form stable complexes with chrysin molecule, which is observed in the experiments [18, 19]. The B orientation is more favorable than S orientation in the structure of β-CD. Binding energies related to various complexes, AB, BB, AS, BS, in gas phase are − 23.79, − 20.62, − 11.16, and − 10.22 kcal/mol, respectively. The more negative value of BE is predicted in solution phase, Table 4. These achieved binding energies indicate that the most probable created complex is AB in both of gas and solution phases. This significant stabilization is due to created hydrogen bonds.

The hydrogen bond here is defined as an O–H…O interaction in which the O…O distance is less than or equal to 3.2 Å and the angle at H atom is greater than 90° [48]. Every intermolecular hydrogen bond stabilized the system about 16–25 kJ/mol [48] in complex between chrysin and β-CD. Therefore, it is important to note that the hydrogen bond interactions play an important role in the binding of chrysin in the β-CD and could be helpful in increasing the stability of the guest/host complex. Position, length and bond angles of hydrogen bonds in AB complex are set in Table 5. Investigation of forming guest/host complex in the most stable complex, AB, indicate that structural details of chrysin, in single molecule,

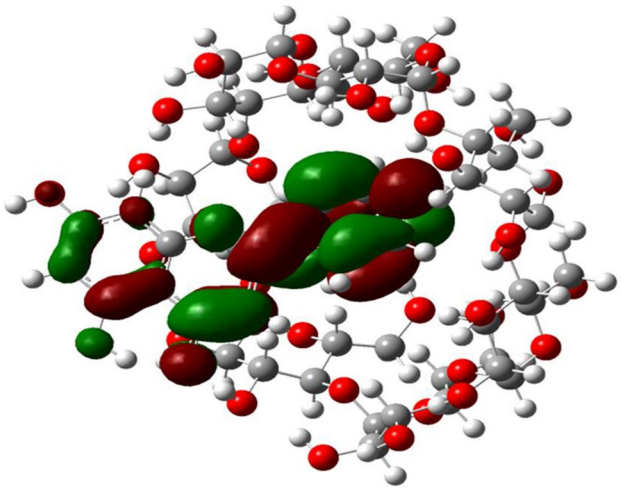

Fig. 7 The highest occupied molecular orbital (HOMO) of AB complex at M05-2x/6–31+G* level in water solution

and in the chrysin/β-CD complex, AB, do not have significant difference. These structural details for chrysin and chrysin/β-CD complex are presented in Table 6, in activate site for chrysin and chrysin/β-CD. Visualizing the HOMO and LUMO chrysin/β-CD in AB complex at M05-2X/6–31+G* level in solution phase shows that the HOMO is more delocalized on the whole of chrysin molecule, as Fig. 7 demonstrates. This delocalization induced more stability in chrysin/β-CD complex rather than chrysin molecule. Calculated HOMO energies for chrysin and chrysin/ β-CD (AB) complex indicate that HOMO energy of AB complex is more stabilized than chrysin in single molecule. HOMO energies for chrysin and chrysin/β-CD (AB) complex are − 7.83 and − 7.84 ev, respectively, at M05-2X/6–31+G* level in solution phase. This stabilization of HOMO confirmed this fact that the chrysin is a good antioxidant compound.

Table 7 Topological properties of AIM for chrysin/β-CD complex (AB) at M05-2X/6–31+G* level in water solvent

The number of α-D-glucopyranoside	Atom of chrysin	Atom of βCD	ρ	$\nabla^2\rho$
1	H(C6)	O(C6)	0.044	−0.035
2	H(O–C7)	O(C6)	0.044	−0.035
3	O(C7)	H(C5)	0.012	−0.010
5	O1	H(C3)	0.006	−0.006
6	O(C4)	H(O–C3)	0.027	−0.023
6	O(C4)	H(C3)	0.010	−0.009
6	O(C5)	H(C3)	0.005	−0.006
6	O(C5)	H(C5)	0.011	−0.009
7	O(C5)	H(C3)	0.006	−0.006
7	O(C5)	H(C5)	0.007	−0.007

AIM analysis

AIM theory is a powerful quantum mechanical formalism for the analysis of theoretical and experimental charge densities, ρ(r). According to AIM theory, each nucleus in a molecule is surrounded by a region mentioned atomic basin that is bounded by a zero-flux surface in ρ that defines an atomic boundary. Previous studies have indicated that when a hydrogen bond is formed, it is associated with the appearance of a bond critical point (bcp) between the hydrogen atom and the acceptor atom [49–51]. This critical point has typical properties of a closed shell interaction. The value of charge density $\rho(r)$ at bond critical point is relatively low and the Laplacian of charge density $\nabla^2\rho(r)$ is positive. This matter indicates that the interaction is dominated by the construction of charge away from the interatomic surface towards each nucleus. The relative large value of charge density at bcp and negative Laplacian charge density indicate that the electronic charge is concentrated in the inter nuclear region. Table 7 shows the topological properties, like charge density and Laplacian of charge density for hydrogen bonds tabulated for chrysin/β-CD complex (AB). In general, for hydrogen bonded complex, the charge density (ρ) and Laplacian of charge density $\nabla^2\rho$ values are in the range of 0.002–0.34 and 0.016–0.13 a.u., respectively, but for hydrogen bond with resonance $\nabla^2\rho$ values is negative [52]. In the present study, the value of (ρ) and ($\nabla^2\rho$) varies from 0.003 to 0.24 and −0.003 to 0.118 a.u., respectively. Therefore, the above values indicate that AB complex is having hydrogen bond with resonance.

Conclusion

In the present work, the B3LYP/6-311++G** method is used to calculate reaction enthalpies related to the free radical scavenging mechanism (HAT) of chrysin. The results indicate that the BDE value for 5-OH group because of internal hydrogen bonding presence is highly thermodynamically unfavorable, so it has the highest value, 87.91 kcal/mol. These results clearly confirm that H transfer is energetically favorable from the A-ring, especially from 7 position and the spin population on the remaining O-atom after H-removal and on the neighboring C-atoms appears to be slightly more delocalized for radicals issued from the A-ring (7-OH position). Therefore, the A-ring is the most important site for H-transfer and consequently for the antioxidant capacity of chrysin. Relative energy values suggest that the reaction between chrysin and hydroxyl radical is exothermic by about −26.66 kcal/mol.

In continuation, the present study depicts the inclusion process of the chrysin in β-cyclodextrin using high-level quantum mechanical calculations. The complex between host (β-CD) and guest (chrysin) was studied from four different orientations: S-ring and B-ring of β-CD with A and B hoop of chrysin. From M05-2x/6–31+G* results, chrysin/β-CD inclusion complex, AB, was predicted to be the most stable structure in both gas and solvent phases. Seven intermolecular hydrogen bonds is formed, a driving force responsible for its stability. Comparison of the complex structures suggests that intermolecular hydrogen bond interactions play an important role in the binding of chrysin in the β-CD complex and also are helpful in increasing the stability of the guest/host complex.

Acknowledgements The authors gratefully acknowledge the research council of Alzahra University for their financial support. The authors would like to appreciate Prof. Hiroshi Sugiyama from Tohoku University for his advices and suggestions for this work.

References

1. R. Challa, A. Ahuja, J. Ali, R.K. Khar, A. A. Pharm. Sci. Tech. **6**, 329 (2005)
2. S.L. Wang, T.W. Yeh, T.I. Ho, Chem. Phys. Lett. **418**, 397 (2006)
3. A. Banerjee, B. Sengupta, S. Chaudhuri, K. Basu, J. Mol. Struct. **794**, 181 (2006)
4. T. Stalin, N. Rajendiran, J. Mol. Struct. **794**, 35 (2006)
5. H. Namazi, Y. Toomari, Adv. Pharml. Bull. **1**, 40 (2011)
6. H. Namazi, S. Bahrami, A.A. Entezami, J. Iran. Polym. **14**, 921 (2005)
7. X. Zhang, Z. Wu, X. Gao, Acta. Biomater. **7**, 585 (2011)
8. K. Jain, P. Kesharwani, U. Gupta, Biomaterials. **33**, 4166 (2012)
9. V. Wintgens, C. Amiel, J. Photo. Chem. A. Chem. **168**, 217 (2004)
10. W. Chen, C.E. Chang, M.K. Gilson, Biophys. J. **87**, 3035 (2004)
11. E.M.M. Del Valle, Process Biochem. **39**, 1033 (2004)

12. D.W. Frank, J.E. Gray, R. Weaver, J. Photo. Chem. A. Chem. **83**, 367 (1976)
13. X. Luo, L. Du, F. He, J. Carbohydr. Chem. **32**, 450 (2013)
14. M. Ghiasi, M. Heravi, Carbohydr. Res. **346**, 739 (2011)
15. G. Zhang, X. Chen, J. Guo, J. Mol. Struct. **921**, 346 (2009)
16. L. Zhou, P. Zhang, G. Yang, R. Lin, W. Wang, T. Liu, L. Zhang, J. Zhang, J. Chem. Eng. Data **59**, 2215 (2014)
17. S. Mahalingam, T. Philip, V. Karuppasamy, J. Kulandaivel, G. Pitchairaj, J. Nanosci. Nanotechnol. **17**, 8742 (2017)
18. S. Samarghandian, J. Tavakkol Afshari, S. Davoodi, Clinics. **66**, 1073 (2011)
19. Z.Y. Zhu, Y. Luo, Y. Liu, X.T. Wang, F. Liu, M.Z. Guo, Z. Wang, A.J. Liu, Y.M. Zang, J. Drug. Deliv. Sci. Technol. **31**, 176 (2016)
20. C. Sandipan, B. Soumalee, L. Ansuman, J. Mol. Struct. **977**, 180 (2010)
21. J. Dobado, N. Benkadour, S. Melchor, J. Mol. Struct. **672**, 127 (2004)
22. N. Al-Rawashdeh, K. Al-Sadeh, M. Al-Bitar, Asian. J. Spectro. **11**, 18 (2013)
23. W. Khuntawee, P. Wolschann, T. Rungrotmongkol, J. Chem. Inf. Model. **55**, 1894 (2015)
24. K. Lipkowitz, Chem. Rev. **98**, 1829 (1998)
25. M. Tafazzoli, M. Ghiasi, Carbohydr. Polym. **78**, 10 (2009)
26. M.J. Frisch, G.W. Trucks, H.B. Schlegel, G.E. Scuseria, M.A. Robb, J.R. Cheeseman, G. Scalmani, V. Barone, B. Mennucci, G.A. Petersson, H. Nakatsuji, M. Caricato, X. Li, H.P. Hratchian, A.F. Izmaylov, J. Bloino, G. Zheng, J.L. Sonnenberg, M. Hada, M. Ehara, K. Toyota, R. Fukuda, J. Hasegawa, M. Ishida, T. Nakajima, Y. Honda, O. Kitao, H. Nakai, T. Vreven, J.A. Montgomery Jr., J.E. Peralta, F. Ogliaro, M. Bearpark, J.J. Heyd, E. Brothers, K.N. Kudin, V.N. Staroverov, R. Kobayashi, J. Normand, K. Raghavachari, A. Rendell, J.C. Burant, S.S. Iyengar, J. Tomasi, M. Cossi, N. Rega, J.M. Millam, M. Klene, J.E. Knox, J.B. Cross, V. Bakken, C. Adamo, J. Jaramillo, R. Gomperts, R.E. Stratmann, O. Yazyev, A.J. Austin, R. Cammi, C. Pomelli, J.W. Ochterski, R.L. Martin, K. Morokuma, V.G. Zakrzewski, G.A. Voth, P. Salvador, J.J. Dannenberg, S. Dapprich, A.D. Daniels, Ö Farkas, J.B. Foresman, J.V. Ortiz, J. Cioslowski, D.J. Fox, *Gaussian 09* (Gaussian, Inc., Wallingford, 2009)
27. F.L. Gainesville, *Hyperchem program, release 7.51 for Windows*. Hypercube Inc., Gainesville
28. I.I.R. Dennington, T. Keith, J. Millam, *Guass view, version 3.09. 2003*. Semichem, Inc., Kansas
29. R.G. Parr, W. Yang, (Oxford Univ. Press, Oxford, 1989)
30. Y. Zhao, D.G. Truhlar, J. Chem. Theory Comput. **1**, 415 (2005)
31. Y. Zhao, N.E. Schultz, D.G. Truhlar, J. Chem. Theory Comput. **2**, 364 (2006)
32. F. Biegler-König, J. Schönbohm, D. Bayles, J. Comp. Chem. **22**, 545 (2001)
33. J. Tomasi, M. Persico, Chem. Rev. **94**, 2037 (1994)
34. V. Barone, M. Cossi, J. Tomasi, J. Chem. Phys. **107**, 3210 (1997)
35. S.B. Boys, F. Bernardi, Mol. Phys. 19 (1970)
36. F.B. Sousa, A.M.L. Denadai, I.S. Lula, Int. J. Pharm. **353**, 160 (2008)
37. Z. Markovic, D. Milenkovic, J. Dorovic, Food. Chem. **134**, 1754 (2012)
38. P. Trouillas, P. Marsal, D. Siri, Food. Chem. **97**, 679 (2006)
39. M. Leopoldini, N. Russo, M. Toscano, Food. Chem. **125**, 288 (2011)
40. J.S. Wright, E.R. Johnson, G.A. DiLabio, J. Am. Chem. Soc. **123**, 1173 (2001)
41. Zh. Velkov, J. Am. Chem. Soc. **123**, 1173 (2001)
42. A. Szabo, N.S. Ostlund, *Modern quantum chemistry: introduction to advanced electronic structure theory* (Dover Publication, New York, 1982)
43. M. Leopoldini, I.P. Pitarch, N. Russo, J. Phys. Chem. A **108**, 92 (2004)
44. C.P. Parkinson, P.M. Mayer, L. Radom, J. Chem. Soc. Perk. Trans. **211**, 2305 (1999)
45. P. Cos, L. Ying, M. Calomme, J. Nat. Prod. **61**, 71 (1998)
46. C. Betzel, B.E. Saenger, G.M. Hingerty, Brown, J. Am. Chem. Soc. **106**, 7545 (1984)
47. L. Nouar, S. Haiahem, B. Abdelaziz, J. Mol. Liq. **160**, 8 (2011)
48. E. Starikov, W. Saenger, T. Steiner, Carbohydr. Res. **307**, 343 (1998)
49. J. Csontos, R. Murphy, S. Lovas, Biopolymers. **89**, 1002 (2008)
50. M.T. Caroll, R.F.W. Bader, Mol. Phys. **65**, 695 (2008)
51. M.T. Caroll, C. Chang, R.F.W. Bader, Mol. Phys. **63**, 387 (1998)
52. G. Gilli, P. Gilli, J. Mol. Struct. **552**, 1 (2000)